COMMUNICATIONS IN NUMERICAL METHODS IN ENGINEERING
Commun. Numer. Meth. Engng 2008; **24**:1315–1323
Published online 17 July 2007 in Wiley InterScience (www.interscience.wiley.com). DOI: 10.1002/cnm.1034

An efficient hourglass control implementation for the uniform strain hexahedron using the Total Lagrangian formulation

Grand Roman Joldes, Adam Wittek and Karol Miller*, †

Intelligent Systems for Medicine Laboratory, School of Mechanical Engineering, The University of Western Australia, 35 Stirling Highway, Crawley/Perth, WA 6009, Australia

SUMMARY

The under-integrated hexahedron is one of the best candidates for use in real-time surgical simulations, because of its computational efficiency. This element requires a very efficient method of controlling the zero energy (hourglass) modes that arise from one-point integration. An efficient implementation of the perturbation hourglass control method proposed by Flanagan and Belytschko for the uniform strain hexahedron is presented. The implementation uses the Total Lagrangian formulation and takes into consideration large deformations and rigid body motions. By using the Total Lagrangian formulation most of the necessary components for calculating the hourglass forces can be pre-computed, leading to a significant reduction of the additional computation time required for hourglass control. The performance evaluation results show the very good accuracy and computational efficiency of the presented algorithm. Copyright © 2007 John Wiley & Sons, Ltd.

Received 14 September 2006; Revised 30 April 2007; Accepted 15 June 2007

KEY WORDS: hourglass control; Total Lagrangian formulation; uniform strain hexahedron; surgical simulation

1. INTRODUCTION

Speed is the main requirement from a finite element model used for surgical simulation. This requirement led many researchers to use linear elastic models, because these models allow to increase the computation speed by applying techniques, such as superposition [1] or static condensation [2–4]. In [5], it is shown that a good material model is crucial for making accurate predictions

*Correspondence to: Karol Miller, Intelligent Systems for Medicine Laboratory, School of Mechanical Engineering, The University of Western Australia, 35 Stirling Highway, Crawley/Perth, WA 6009, Australia.
†E-mail: kmiller@mech.uwa.edu.au

Contract/grant sponsor: Australian Research Council, Discovery Project; contract/grant numbers: DP0343112, DP0664534, LX0560460
Contract/grant sponsor: NIH; contract/grant number: 1-RO3-CA126466-01A1

on tissue deformations and Picinbono *et al.* [6] and Wittek *et al.* [7] demonstrate the shortcoming of linear elasticity when rigid body motions are present. As tissue deformations during surgery are large and material properties of biological tissues are highly nonlinear [8–11], we can draw the conclusion that nonlinear material laws and nonlinear finite element models should be used in order to have accurate results.

In a previous paper, we presented a very efficient Total Lagrangian Explicit Dynamics (TLED) algorithm for computing soft tissue deformations, with application to real-time surgical simulation [12]. This algorithm can be used for nonlinear models with any material law or element type. We demonstrated that the Total Lagrangian formulation has advantages over the Updated Lagrangian formulation from the computational point of view. This algorithm is capable of computing a time step in 16 ms for a mesh having 6000 elements and 6741 nodes on a standard Pentium 4. It is clear that improvements in the algorithm and computing hardware can make real-time computations possible.

This paper presents algorithmic improvements related to hourglass control. In order to meet the speed requirements, the finite element models must use computationally inexpensive low-order elements such as the linear under-integrated hexahedron or the linear tetrahedron. The single integration point first-order hexahedral finite elements can also be used with materials having high Poisson's ratio because they do not exhibit volumetric locking [13]. But these elements also require the use of an hourglass control algorithm in order to eliminate the zero energy modes that arise from one-point integration [14]. We will show that the Total Lagrangian formulation is recommended from the point of view of efficient hourglass control implementation, as many quantities involved can be pre-computed.

One of the earliest and most popular hourglass control algorithms that is currently available in many commercial software finite element packages (ABAQUS [15], LS-DYNA [16]) is the one proposed by Flanagan and Belytschko [14], also known as the perturbation hourglass control. This method is applicable for hexahedral elements with arbitrary geometry used for the simulation of large deformations (including rigid body motions).

Several other algorithms were proposed for hourglass control. Liu *et al.* [17] proposed the usage of stabilization matrices for hourglass control in the so-called physical stabilization method. The algorithm required the storage of 36 hourglass stresses in addition to the single-point stresses and the resulting stabilization forces causes the element to experience volumetric and shear locking [18].

Belytschko and Bindeman [19] proposed an assumed strain stabilization method and Puso [18] combined the physical stabilization method with the assumed strain method in order to obtain an efficient enhanced assumed strain physically stabilized element. These methods provide an improved behavior of the element in bending-dominated problems. However, the stability of these methods cannot be guaranteed for general deformation states and arbitrarily shaped elements [20]. The enhanced strain physically stabilized element is also available in the commercial finite element codes [15, 16].

In the context of large deformations, rigid body motions and arbitrarily shaped elements, the perturbation hourglass control is the most computationally efficient of the presented hourglass control methods. The increased performance of the enhanced assumed strain hourglass control methods in bending-dominated problems is of little importance in surgical simulation.

The remainder of the paper is organized as follows. The improved algorithm for the computation of hourglass control forces is presented in Section 2. Performance of the algorithm is assessed using two numerical simulations in Section 3. Discussion and the conclusions are presented in Section 4.

DOI: 10.1002/cnm

2. COMPUTATION OF HOURGLASS CONTROL FORCES

The notation from [13], also used in our previous paper [12], is used, where the left superscript represents the current time and the left subscript represents the time of the reference configuration, which is 0 when Total Lagrangian formulation is used.

Based on the relations presented in [14], the following quantities can be defined with respect to the original configuration (using indicial notation):

- The mean shape functions derivatives, for the uniform strain hexahedron

$$ {}_0\bar{h}_{I,i} = \frac{B_{Ii}}{V} = \frac{1}{V}\int_V {}_0h_{I,i}\,\mathrm{d}V, \quad I = 1\ldots 8, \quad i = 1\ldots 3 \tag{1} $$

  where the B-matrix and the element volume V are computed as presented in [14].
- The hourglass shape vectors

$$ {}_0\gamma_{I\alpha} = \Gamma_{I\alpha} - \frac{1}{V} B_{Ii}\,{}^0x_{Ji}\Gamma_{J\alpha} = \Gamma_{I\alpha} - {}_0\bar{h}_{I,i}\,{}^0x_{Ji}\Gamma_{J\alpha}, \quad \alpha = 1\ldots 4, \quad I = 1\ldots 8 \tag{2} $$

  where $\Gamma_{I\alpha}$ are the constant hourglass base vectors and ${}^0x_{Ji}$ are the initial nodal coordinates (see [14]).
- The hourglass nodal velocities

$$ {}^t_0\dot{q}_{\alpha i} = \frac{1}{\sqrt{8}}\,{}^t_0\dot{u}_{Ii}\,{}_0\gamma_{I\alpha} \tag{3} $$

  where ${}^t_0u_{Ii}$ are the nodal displacements with regard to the original configuration.
- The hourglass resistance for the artificial stiffness is given in terms of the maximum stiffness of the element $K_{\max}$

$$ {}^t_0Q_{\alpha i} = \kappa \cdot K_{\max} \cdot {}^t_0q_{\alpha i} \tag{4} $$

  where κ is a user-defined stiffness parameter.
- The contribution of the hourglass resistance to the nodal forces

$$ {}^t_0f^{\mathrm{Hg}}_{Ii} = \frac{1}{\sqrt{8}}\,{}^t_0Q_{\alpha i}\,{}_0\gamma_{I\alpha} \tag{5} $$

For a lumped mass matrix in which the mass is distributed equally among the 8 nodes (usually used in an explicit analysis), the maximum stiffness is related to the maximum element frequency $\omega_{\max}$ by

$$ K_{\max} = \frac{\rho V}{8}\omega^2_{\max} \tag{6} $$

where ρ is the density.

An estimate of the maximum element frequency is used, as given in [21]

$$ \omega_{\max} \leqslant c_{\mathrm{D}} \cdot g^{1/2} \tag{7} $$

DOI: 10.1002/cnm

where c_D is the dilatational wave velocity in the material and g is the geometrical parameter. In the case of a hexahedron with arbitrary configuration, g is given in [14] as

$$g = 8\frac{B_{Ii}B_{Ii}}{V^2} = 8\,{}_0\overline{h}_{I,i}\,{}_0\overline{h}_{I,i} \tag{8}$$

When the Lame material parameters λ and μ are known, the dilatational wave velocity can be expressed as

$$c_D = \sqrt{\frac{\lambda + 2\mu}{\rho}} \tag{9}$$

From the above relations it can be seen that the mean shape function derivatives and the hourglass shape vectors are constant when they are defined with respect to the initial configuration and can be pre-computed. A further simplification can be obtained by integrating (3) with zero initial conditions for displacements and hourglass nodal displacements

$$ {}_0^t u_{Ii} = 0 \quad \text{and} \quad {}_0^t q_{\alpha i} = 0 \tag{10}$$

The zero initial conditions are obtained from the fact that when the nodal displacements ${}_0^t u_{Ii}$ are zero, the hourglass nodal displacements ${}_0^t q_{\alpha j}$ are also zero, and therefore no hourglass resistance force is present. After integration we obtain

$$ {}_0^t q_{\alpha i} = \frac{1}{\sqrt{8}}\,{}_0^t u_{Ii}\,{}_0\gamma_{I\alpha} \tag{11}$$

If we use the following notation:

$$k = \frac{\kappa \cdot K_{\max}}{8} \tag{12}$$

and replace (4), (11) and (12) in (5), the hourglass resistance forces will become

$$ {}_0^t f_{Ii}^{\mathrm{Hg}} = k\,{}_0^t u_{Ji}\,{}_0\gamma_{J\alpha}\,{}_0\gamma_{I\alpha} \tag{13}$$

Written in the matrix form, relation (13) becomes

$$ {}_0^t \mathbf{F}^{\mathrm{Hg}} = k\,{}_0\boldsymbol{\gamma}\,{}_0\boldsymbol{\gamma}^{\mathrm{T}}\,{}_0^t\mathbf{u} \tag{14}$$

where $\boldsymbol{\gamma}$ is the matrix of hourglass shape vectors and $\mathbf{u}$ is the matrix of displacements.

In (14) all the involved quantities, except the displacements, are constant and can be pre-computed. Therefore, the computation of the hourglass control forces in a Total Lagrangian framework becomes very efficient, requiring only 360 floating point operations per element. An estimation of the number of operations required for implementing the same algorithm (relations 1–14) in an Updated Lagrangian framework is given in Table I. When the Total Lagrangian formulation is used instead of Updated Lagrangian, the number of floating point operations per element reduces by a factor larger than 4.

3. PERFORMANCE EVALUATION

In order to assess the performances of the proposed hourglass control mechanism, its implementation was included in the TLED algorithm presented in [12]. This algorithm was used to conduct two

DOI: 10.1002/cnm

Table I. Number of floating point operations per element required for the implementation of the proposed hourglass control algorithm when using different formulations.

Formulation	Total Lagrangian	Updated Lagrangian
Number of floating point operations	360	1585

numerical experiments, which include large deformations, rigid body motions and elements with arbitrary geometry: indentation of an ellipsoid (that coarsely resembles the brain) and deformation of a column.

In both the experiments the loading was imposed by displacing selected nodes on the surface. The displacements were applied using a smooth loading curve given by

$$d(t) = d_{\max} \cdot (10 - 15t + 6t^2) \cdot t^3 \tag{15}$$

where t is the relative time (varying from 0 to 1).

The simulation results were compared with the results obtained using the commercial finite element software ABAQUS [22]. Fully integrated linear hexahedra, hybrid displacement–pressure formulation, were used in ABAQUS. Because these elements do not exhibit hourglassing or volumetric locking in the case of almost incompressible materials, the obtained results were considered as the 'golden standard' for comparison. The results were obtained using the implicit solver with the default configuration.

3.1. *Indentation of an ellipsoid*

We presented an ellipsoid indentation experiment in our previous paper [12], used for assessing the accuracy of the TLED algorithm. A similar experiment is presented here, but this time we used the asymmetric loading and much larger deformations in order to excite the hourglass modes of the elements. If no hourglass control is used, the simulation leads to very unrealistic results.

The ellipsoid presented in Figure 1 was deformed by constraining a part of the lower surface ($\Delta x = \Delta y = \Delta z = 0$) and displacing selected nodes from the upper surface ($\Delta x = 0, \Delta y = 0, \Delta z = d_z(t)$), with maximum displacements of 0.04 m in the z direction. The mesh was constructed using Altair HyperMesh [23] and has 2535 nodes and 2200 elements with arbitrary geometry.

A Neo-Hookean almost incompressible material model was used, having the mechanical properties similar to those of the brain (mass density of $1000\,\mathrm{kg/m^3}$, Young's modulus in undeformed state equal to 3000 Pa and Poisson's ratio 0.49).

The comparison of displacements of nodes located on the surface and in the plane $y = 0$ is presented in Figure 2.

3.2. *Deformation of a column*

This experiment was artificially designed to compound difficulties associated with hourglass control: large deformations, bending and rigid body motions. A column having a height of 1 m and a square section with the side size 0.1 m was meshed using hexahedral elements (Figure 3(a)). The mesh has 496 nodes and 270 elements. The material properties were the same as those used in the previous experiment.

DOI: 10.1002/cnm

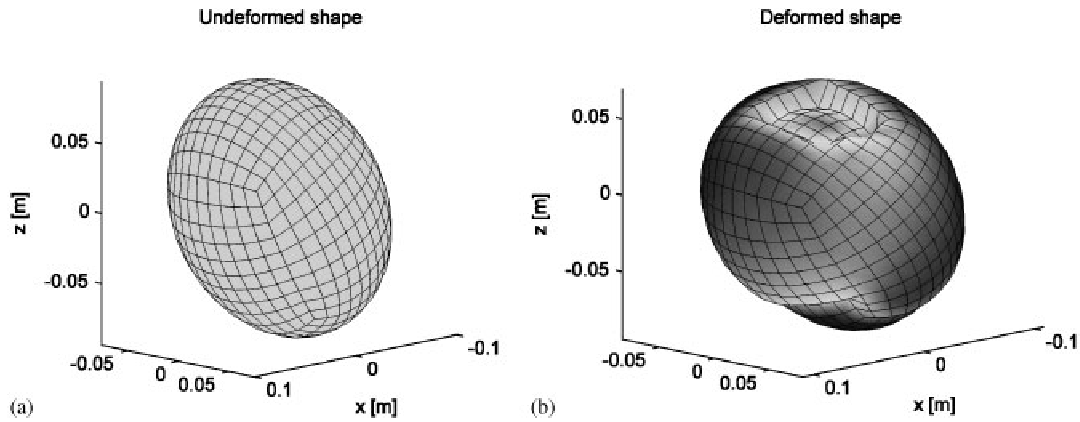

Figure 1. Indentation of an ellipsoid—undeformed shape (a) and deformed shape (b).

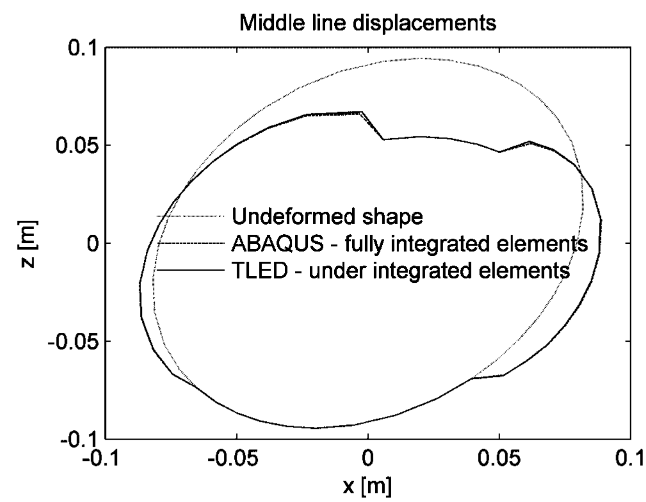

Figure 2. Indentation of an ellipsoid—middle line displacements.

The deformation was imposed by constraining the lower face ($\Delta x = \Delta y = \Delta z = 0$) and displacing the upper face ($\Delta x = d_x(t)$, $\Delta y = 0$, $\Delta z = d_z(t)$), with maximum displacements of 0.5 m in the x direction and 0.3 m in the z direction.

The deformed shape obtained using the TLED algorithm is presented in Figure 3(b) for the case when under-integrated hexahedral elements with no hourglass control are used. The influence of the presented hourglass control mechanism can be clearly seen in Figure 3(c).

The comparison of displacements of a line of nodes from the side of the column (in the plane $y = 0$) is presented in Figure 4.

Very good agreement between the results obtained using the under-integrated elements with the presented hourglass control and the fully integrated linear hexahedra with hybrid displacement–pressure formulation can be observed. The displacement maximum relative error, defined as the

DOI: 10.1002/cnm

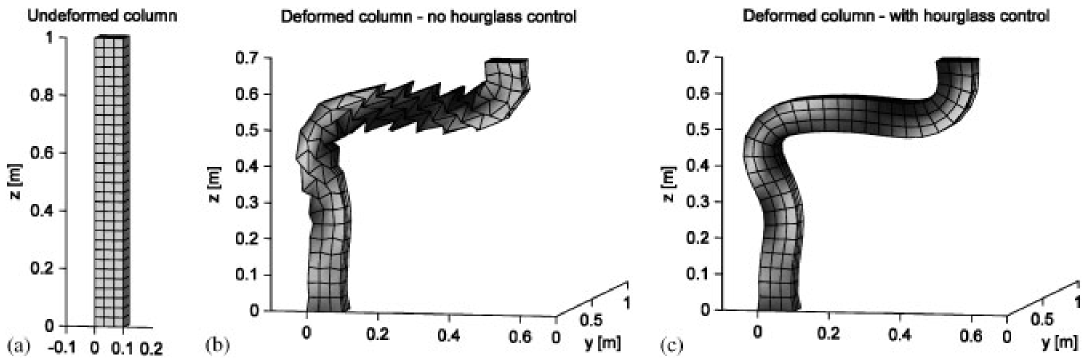

Figure 3. Deformation of a column—undeformed shape (a), deformed shape with no hourglass control (b) and deformed shape with successful hourglass control (c).

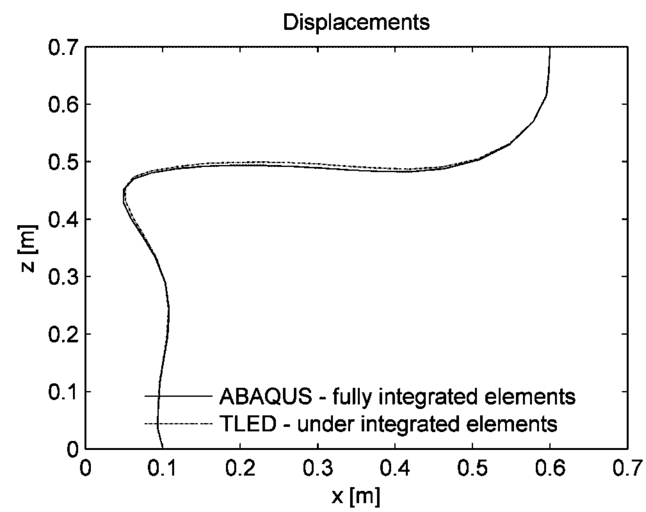

Figure 4. Deformation of a column—middle line displacements.

ratio between the maximum displacement difference and the imposed displacement, was 0.34% in the case of ellipsoid indentation and 1.4% in the case of column deformation. This demonstrates the good accuracy of the elements using the proposed hourglass control mechanism.

Table II presents the computation time required for running one time step in an explicit analysis when using different hourglass control mechanisms in the Total Lagrangian and Updated Lagrangian frameworks. The ellipsoid indentation simulation was used for time measurement. The presented hourglass control method was compared with two other methods available in ABAQUS Explicit. The first is basically the same perturbation-based stiffness hourglass control, but implemented in the Updated Lagrangian framework. The second is an enhanced assumed strain hourglass control method. A fixed time step and no output requests were used in order to eliminate other influences on the computation time. Because the usage of Total Lagrangian or Updated Lagrangian

DOI: 10.1002/cnm

Table II. Computation time required for running one time step using under-integrated hexahedra with different hourglass control methods and different frameworks (ellipsoid indentation simulation—2535 nodes and 2200 elements).

	Perturbation-based stiffness		
Hourglass control method	Total Lagrangian framework	Updated Lagrangian framework	Enhanced assumed strain, Updated Lagrangian framework
Software used	TLED	ABAQUS explicit	ABAQUS explicit
Computation time (ms)	2.1	10.6	13.7

does not influence the critical time step [13], the same step size and number of steps can be used for all analyses and we can compare the computation time required for only one time step.

The simulation results demonstrate the computational efficiency of the under-integrated hexahedral element with perturbation-based stiffness hourglass control in the case of Total Lagrangian framework. They also demonstrate the known fact that the enhanced assumed strain hourglass control is more computationally expensive than the perturbation-based stiffness hourglass control.

4. CONCLUSIONS

A very efficient implementation of the stiffness-based hourglass control mechanism described in [14] in the case of a Total Lagrangian computational framework is presented in this paper. By referring all the components necessary for computing the hourglass control forces to the original configuration, they can be pre-computed and therefore only a few operations are required at every time step for the hourglass control mechanism.

The influence of the hourglass control mechanism on the simulation results is clearly visible. In order to assess the accuracy of the computation results, they were compared with the results obtained using mixed formulation fully integrated elements and the commercial finite element software (ABAQUS). A very good agreement of the results was obtained.

Our under-integrated hexahedral element using perturbation-based stiffness hourglass control is almost five times more computationally efficient in the Total Lagrangian framework than in the Updated Lagrangian framework. This demonstrates the need to consider the Total Lagrangian framework for real-time surgical simulations.

ACKNOWLEDGEMENTS

The first author was an IPRS scholar in Australia during the completion of this research. The financial support of the Australian Research Council (grant nos. DP0343112, DP0664534 and LX0560460) and NIH (grant nos. 1-RO3-CA126466-01A1) is gratefully acknowledged. We would like to thank Prof. Graham Carey for very helpful discussions during his visit to Perth in July 2006.

REFERENCES

1. Cotin S, Delingette H, Ayache N. Real-time elastic deformations of soft tissues for surgery simulation. *Transactions on Visualization and Computer Graphics* 1999; **5**(1):62–73.

DOI: 10.1002/cnm

2. Bro-Nielsen M, Cotin S. Real-time volumetric deformable models for surgery simulation using finite elements and condensation. *Computer Graphics Forum* 1996; **15**(3):57–66.
3. Bro-Nielsen M. Finite element modeling in surgery simulation. *Proceedings of the IEEE* 1998; **86**(3):490–503.
4. DiMaio SP, Salcudean SE. Needle insertion modelling and simulation. *Proceedings of IEEE International Conference on Robotics and Automation,* Washington, U.S.A., 11–15 May, 2002; 2098–2105.
5. Nienhuys H-W, van der Stappen AF. A computational technique for interactive needle insertions in 3D nonlinear material. *IEEE International Conference on Robotics and Automation* (*ICRA*), New Orleans, LA, 2004.
6. Picinbono G, Delingette H, Ayache N. Non-linear anisotropic elasticity for real-time surgery simulation. *Graphical Models* 2003; **65**:305–321.
7. Wittek A, Miller K, Kikinis R, Warfield SK. Patient-specific model of brain deformation: application to medical image registration. *Journal of Biomechanics* 2007; **40**:919–929.
8. Miller K, Chinzei K. Mechanical properties of brain tissue in tension. *Journal of Biomechanics* 2002; **35**:483–490.
9. Miller K, Chinzei K, Orssengo G, Bednarz P. Mechanical properties of brain tissue in-vivo: experiment and computer simulation. *Journal of Biomechanics* 2000; **33**:1369–1376.
10. Miller K. Constitutive modelling of abdominal organs (Technical note). *Journal of Biomechanics* 2000; **33**: 367–373.
11. Miller K, Chinzei K. Constitutive modelling of brain tissue; experiment and theory. *Journal of Biomechanics* 1997; **30**(11–12):1115–1121.
12. Miller K, Joldes GR, Lance D, Wittek A. Total Lagrangian explicit dynamics finite element algorithm for computing soft tissue deformation. *Communications in Numerical Methods in Engineering* 2007; **23**:121–134.
13. Bathe K-J. *Finite Element Procedures*. Prentice-Hall: Englewood Cliffs, NJ, 1996.
14. Flanagan DP, Belytschko T. A uniform strain hexahedron and quadrilateral with orthogonal hourglass control. *International Journal for Numerical Methods in Engineering* 1981; **17**:679–706.
15. *ABAQUS/Explicit User's Manual Version 6.1*. Hibbitt, Karlsson & Sorensen, Inc.: Pawtucket, 2000.
16. Hallquist JO. *LS-DYNA Theory Manual*. Livermore Software Technology Corporation: Livermore, CA, 2005.
17. Liu WK, Ong JS-J, Uras RA. Finite element stabilization matrices—a unification approach. *Computer Methods in Applied Mechanics and Engineering* 1985; **53**(1):13–46.
18. Puso MA. A highly efficient enhanced assumed strain physically stabilized hexahedral element. *International Journal for Numerical Methods in Engineering* 2000; **49**:1029–1064.
19. Belytschko T, Bindeman LP. Assumed strain stabilization of the eight node hexahedral element. *Computer Methods in Applied Mechanics and Engineering* 1993; **105**:225–260.
20. Reese S, Wriggers P. A stabilization technique to avoid hourglassing in finite elasticity. *International Journal for Numerical Methods in Engineering* 2000; **48**:79–109.
21. Hughes TJR. Analysis of transient algorithms with particular reference to stability behavior. In *Computational Methods for Transient Analysis*, Belytschko T, Hughes TJR (eds). New-Holland: Amsterdam, 1983; 67–155.
22. ABAQUS. *ABAQUS Theory Manual*, *Version 5.8*. Hibbitt, Karlsson & Sorensen, Inc., 1998.
23. Altair HyperMesh. http://www.uk.altair.com/software/hypermesh.htm [June 2006].

DOI: 10.1002/cnm